SPE 164797

A Novel Infinite-Acting Radial-Flow Analysis Procedure for Estimating Horizontal and Vertical Permeability from an Observation-Probe Pressure Response

M. Onur, SPE, UniversitiTeknologi PETRONAS, P.S. Hegeman,Schlumberger, and I.M. Gok, SPE, Schlumberger

This paper was prepared for presentation at the EAGE Annual Conference & Exhibition incorporating SPE Europec held in London, United Kingdom, 10–13 June 2013.

Abstract

This paper presents a new infinite-acting radial-flow analysis procedure for estimating horizontal and vertical permeability solely from pressure transient data acquired at an observation probe during an interval pressure transient test (IPTT) conducted with a single-probe or dual-packer module. The procedure is based on new infinite-acting radial-flow equations that apply for all inclination angles of the wellbore in a single-layer, 3D anisotropic, homogeneous porous medium. The equations for 2D anisotropic cases are also presented and are derived from the general equations given for the 3D anisotropic case. It is shown that the radial-flow equation presented reduces to the Prats' equation assuming infinite-acting radial flow at an observation point along a vertical wellbore in isotropic or 2D anisotropic formations of finite bed thickness.

The applicability of the analysis procedure is demonstrated by considering synthetic and field probe-probe and packer-probe IPTT data. The results indicate that the procedure provides reliable estimates of horizontal and vertical permeability solely from observation-probe pressure data during radial flow for vertical, horizontal, and slanted wellbores. Most importantly, the analysis does not require that both spherical and radial flow prevail at the observation probe during the test.

Introduction

Permeability and permeability anisotropy are some of the most important parameters for both reservoir management and well performance. Permeability and its anisotropy strongly affect all reservoir displacement processes. Thus, estimation of the individual values of horizontal and vertical permeability is becoming increasingly important as emphasis shifts from primary to secondary and tertiary recovery. Interval pressure transient testing (IPTT) using packer-probe or probe-probe wireline formation testers provides dynamic permeability and anisotropy information with increased vertical resolution along the wellbore. The test can be conducted by withdrawing fluid with a single-probe formation testing tool (**Fig. 1**) or a dual-packer formation testing tool(**Figs. 2** and **3**) (e.g., see Zimmerman et al. 1990; Goode and Thambynayagam 1992; Pop et al. 1993; Kuchuk et al. 1994). Fig. 1 shows a schematic of an observation probe with a singleprobe flowing (or simply, a sink probe), whereas Fig. 2 is a schematic for a dual-packer module. In these figures the wellbore is vertical. (For more information on the terms "vertical" and "horizontal," see Appendix A entitled as "Terminology.") Fig. 3 illustrates the case of a dual-packer module in an inclined wellbore; likewise, the single-probe module can be deployed in an inclined well (not shown).

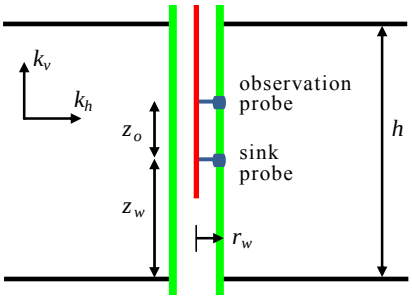

Fig. 1—Schematic diagram of a single-probe tool with an observation probe in a vertical wellbore.

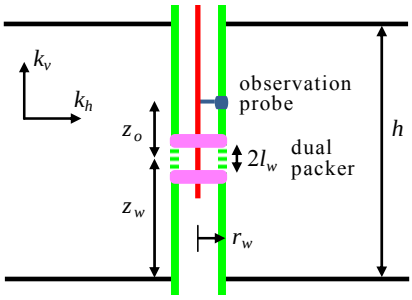

Fig. 2—Schematic diagram of a dual-packer tool with an observation probe in a vertical wellbore.

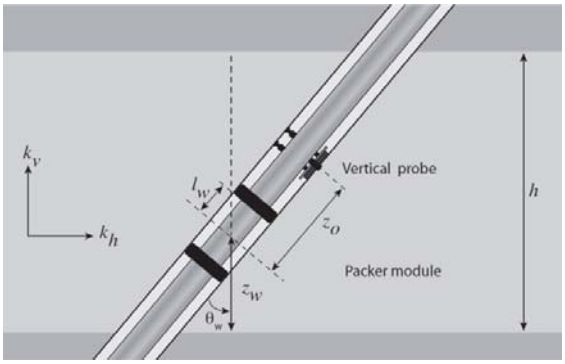

Fig. 3—Schematic diagram of a dual-packer tool with an observation probe in an inclined wellbore.

The transient pressure response at an observation probe during an IPTT has been studied in great detail for the case of an unbounded formation in the vertical direction (i.e., spherical flow). For example, Zimmerman et al. (1990) and Goode and Thambynayagam (1992) describe methods to determine horizontal (k_h) and vertical permeability (k_v) from observation-probe spherical-flow response when flowing through a single-probe tool. Their methods require two observation probes—one positioned on the opposite side of the borehole on the same horizontal plane as the sink probe and the other displaced vertically on the same azimuthal plane as the sink probe. Although Goode and Thambynayagam present an analytical equation for the case of a finite-thickness formation, they do not provide any method to use the equation to determine permeability. Furthermore, they do not disclose methods for the case of flow through a dual-packer tool. Onur et al. (2011) describe a method to determine horizontal and vertical permeability from observation-probe spherical-flow response when flowing through a dual-packer tool.

For the case of finite bed thickness, the resulting radial (or pseudoradial) flow response at the observation probe has received less attention. However, field tests show that observation-probe data often do not exhibit a spherical-flow regime in thinly laminated formations, but instead show only a radial-flow regime.

This paper provides a new infinite-acting radial-flow analysis method to determine the horizontal and vertical permeability from the radial-flow response at an observation probe of an IPTT. The method applies for tests conducted with a single-probe tool (Fig. 1) ora dual-packer tool (Figs. 2 and 3). It is based on an adaptation of a well-testing method presented by Prats (1970) for vertical wells with 2D permeability anisotropy. We have extended the method to the general case of an inclined wellbore in a reservoir with 3D permeability anisotropy by applying Besson (1990) transformationsto the Prats' equation for the isotropic system. This resulted in new infinite-acting radial-flow equations that apply for all inclination angles of the wellbore in a single-layer, 3D anisotropic, homogeneous porous medium. The equations for 2D anisotropic cases are also presented and are derived from the general equations given for the 3D anisotropic case. The wellbore inclination can range from 0° (vertical) to 90° (horizontal). Furthermore, Prats developed his method for the case of producing (injecting) the well at a constant flow rate. However, in practice, it can be difficult to maintain a constant rate; thus, we have adapted the method for the case where the production period is followed by a buildup test.

In the wireline formation-testing (WFT) literature, to the best of our knowledge, such an analysis method and equations have not been presented. Therefore, the new analysis procedure and the new equations presented in this paper should be useful for estimating horizontal and vertical permeability from WFT observation-probe pressure data exhibiting a radial-flow regime.

Method of Prats for Vertical Interference Testing

In the well-testing literature, Prats (1970) described a method for determining vertical permeability in a single-layer system with no-flow top and bottom boundaries. He proposed withdrawing or injecting fluid through a single perforation as a way to obtain vertical flow in the formation. Furthermore, he proposed using a second perforation, separated from the first by a casing packer, to measure the vertical pressure response. Prats modeled the producing perforation as a point source on the surface of a well of zero radius. The well completion is illustrated in **Fig. 4**. Prats studied only the case of a vertical well ($\theta_w=0°$) with 2D permeability anisotropy (i.e., $k_h \neq k_v$); furthermore, he assumed that the flowing perforation produces at a constant rate of flow.

Drawdown Test. Prats showed that the late-time (infinite-acting radial flow) pressure response at the observation perforation due to constant-rate production from the producing perforation is given by

$$p_{i,o} - p_{wf,o}(t) = m \log t + b, \quad \text{..... (1)}$$

where

$$m = 162.6 \frac{q\mu}{k_h h} \quad \text{..... (2)}$$

and

$$b = 162.6\frac{q\mu}{k_h h}\left[\frac{G^* + h/|\Delta Z_R|}{2.303} + \log\left(\frac{0.0002637 k_v}{\phi\mu c_t h^2}\right)\right]. \quad (3)$$

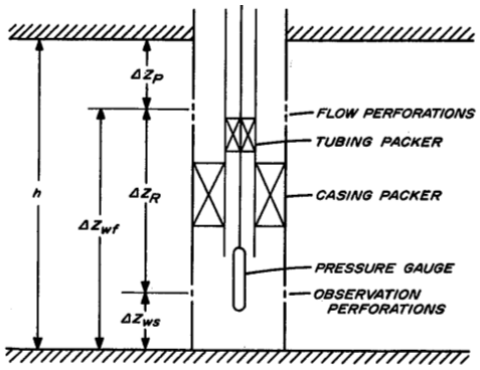

Fig. 4—Well completion for a vertical interference test (Earlougher 1977, 1980).

The flow rate, q, is positive for a production period and negative for an injection period. In Eq. 3 G^* is the geometrical function provided by Prats. G^* depends on the position of the production (injection) and measuring perforations with respect to the vertical boundaries of the reservoir. G^* is given by

$$G^* = \frac{1}{Z + Z'} - 2\ln 2 - \gamma - \frac{1}{2}\sum_{i=1}^{4}\Psi\left(\frac{a_i + 1}{2}\right) \quad (4)$$

where $Z = \Delta Z_{ws}/h$, $Z' = \Delta Z_{wf}/h$, and

$$a_1 = 1 + Z + Z';\ a_2 = 1 + Z - Z';\ a_3 = 1 - Z + Z';\ a_4 = 1 - Z - Z'. \quad (5)$$

Thus, G^* is a function of only Z and Z', which are the dimensionless positions of the observation and active perforations, respectively. G^* is a symmetric function—that is, $G^*(Z, Z') = G^*(Z', Z)$. This property is sometimes referred to as the "reciprocity principle," which states that the pressure response between two points is independent of the direction of flow between them (McKinley et al. 1968; Carter et al. 1974). The digamma function, Ψ (also referred to as the "psi function"), in Eq. 4 can be evaluated using an algorithm by Codyet al. (1973). **Fig. 5** presents a graph of G^* as a function of$\Delta Z_{ws}/h$ and $\Delta Z_{wf}/h$.

For a constant-rate test at the producing perforation, Eq. 1 indicates that a semilog plot of pressure at the observation perforation vs. time, $p_{wf,o}$ vs. log t, yields a straight line with slope $-m$ and intercept $p_{wf,o}(t=1)$. From these straight-line parameters we can compute

$$k_h = 162.6\frac{q\mu}{mh} \quad (6)$$

and

$$k_v = \frac{\phi\mu c_t h^2}{0.0002637}10^{\alpha}, \quad (7)$$

where

$$\alpha = \frac{p_{i,o} - p_{wf,o}(t=1)}{m} - \frac{G^* + h/|\Delta Z_R|}{2.303}. \quad (8)$$

Buildup Test. Prats developed his method for the case of producing (injecting) the well at a constant flow rate. However, in practice, it can be difficult to maintain a constant rate; thus, an alternate method of testing is to follow the production period with a buildup test. For a buildup test (i.e., the well is shut in and flow rate $q=0$) following a constant-rate test, the late-time (infinite-acting radial flow) pressure response at the observation perforation can be computed from the superposition of two constant-rate drawdown solutions:

$$p_{ws,o}(\Delta t) = p_{i,o} - m\log\left(\frac{t_p + \Delta t}{\Delta t}\right). \quad (9)$$

Another useful form of the superposition equation is obtained by subtracting the drawdown solution evaluated at time $t = t_p$ from the buildup pressure response:

$$p_{ws,o}(\Delta t) - p_{wf,o}(t_p) = m \log\left(\frac{t_p\,\Delta t}{t_p + \Delta t}\right) + b\,. \quad (10)$$

Eq. 9 indicates that a semilog plot of buildup pressure at the observation perforation vs. Horner time, $p_{ws,o}$ vs. log $[(t_p+\Delta t)/\Delta t]$, yields a straight line with slope $-m$ and intercept $p_{i,o}$. We can then compute k_h from the slope using Eq. 6. We can evaluate Eq. 10 at any desired value of Δt, and then solve for k_v. A convenient choice is $\Delta t = 1$ hour, and the result is

$$k_v = \frac{\phi\mu c_t h^2}{0.0002637}\,10^{\beta}\,, \quad (11)$$

where

$$\beta = \frac{p_{ws,o}(\Delta t = 1) - p_{wf,o}(t_p)}{m} - \frac{G^* + h/|\Delta Z_R|}{2.303} + \log(1 + 1/t_p)\,. \quad (12)$$

In Eq. 12, $p_{ws,o}(\Delta t = 1)$ must be evaluated from the straight line.

For test conditions that are more complex than a constant flow rate, or constant flow rate followed by a buildup, the superposition method as demonstrated here can be extended to account for any flow rate condition. To eliminate variable-rate effects even more rigorously, we can use recently proposed pressure/rate deconvolution methods to convert the observation-probe data to equivalent constant-rate data (von Schroeteret al. 2004; Onur et al. 2008; Pimonovet al. 2010).

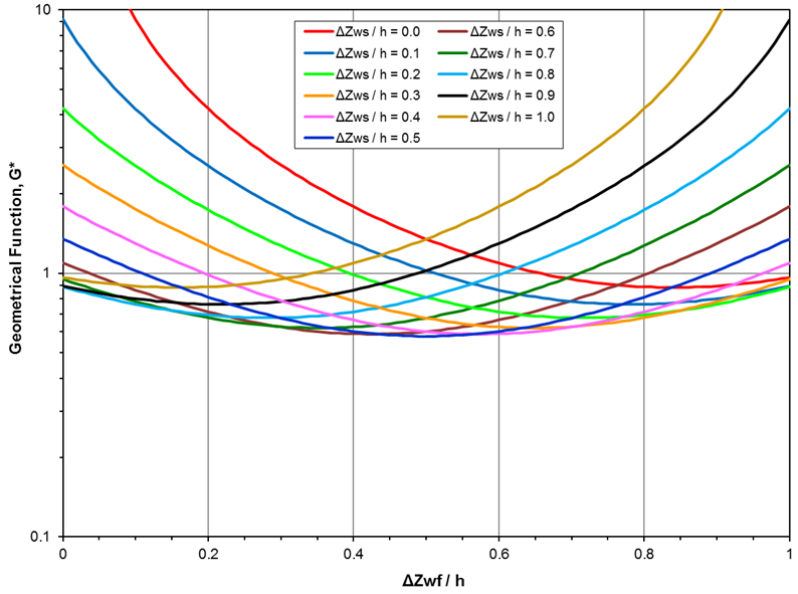

Fig.5—Geometrical function computed with Eq. 4.

Discussion and Limitations of Prats' Method. In the context of a well-testing method, Prats (1970) noted several requirements for the test:

1. The well must have casing and must be cemented behind the casing.
2. There must be no communication through the cement behind the casing. [Earlougher (1980) states that a microannulus only 0.001-in. wide can give enough vertical flow between the producing and observation perforations to cause the appearance of a high vertical permeability.]
3. The producing and observation locations must not be in communication through the wellbore (which means they must be separated by a casing packer or plug).
4. The test must be conducted long enough to achieve radial flow; the pressure response at the observation location must be large enough to be measured during the test duration.
5. Although the method is derived for single perforations at the producing and observation locations, finite-length intervals may be used. In such cases, the producing and observation intervals must be short compared with the distance between them, probably 10% or less.
6. The analysis method is based on the assumption of a zero-radius (i.e., line-source) well. For the method to apply to a finite-radius wellbore,

$$|\Delta Z_R| > 25 r_w \sqrt{k_v / k_h}\,. \quad (13)$$

Earlougher (1980) states that simulations show that the constant in the right-hand side of Eq. 13 can be relaxed to about 12 instead of 25 (although he erroneously omits the square root sign). Furthermore, as noted previously, Prats studied only the case of a vertical well (θ_w=0°) with the flowing perforation producing at a constant rate of flow.

Adaptation of Prats' Method to Wireline Formation Testing

Although Prats' method was developed for well-testing applications, an IPTT as illustrated in Figs. 1–3 typically meets most of the requirements of the method. An IPTT is usually conducted in open hole; thus, the requirements for casing and good cement are replaced by a requirement for a sealing mudcake. For a dual-packer IPTT test, there may be an issue with the length of the flowing interval exceeding 10% of the distance between the packer and observation probe. For both a probe test and a dual-packer test, there may be an issue with the requirement of Eq. 13.

To evaluate Prats' method for analysis of pressure data acquired at an IPTT observation probe, a number of synthetic cases have been analyzed; we present four cases here. All synthetic cases have been generated with the analytical solutions of Kuchuk (1996) for a single-probe tool (Fig. 1) and Kuchuk (1994) for the dual-packer tool (Fig.2) for a vertical well.The correspondence between Prats' terminology and the WFTs of Figs. 1 and 2 is $\Delta Z_{wf} = z_w$, $\Delta Z_{ws} = z_w + z_o$, and $\Delta Z_R = z_o$.

Case 1. Single-Probe Tool, with $k_h > k_v$. The input data used to generate this case are $h = 20$ ft, $k_h = 100$ md, $k_v = 10$ md, $z_w = 8$ ft, $z_o = 2.3$ ft, $\mu = 0.5$ cp, $\phi = 0.2$, $c_t = 8\times10^{-6}$ 1/psi, $p_{i,o} = 5000$ psi, $r_p = 0.22$ in, and $r_w = 0.25$ ft. The test sequence comprised a 2-hr flow at 14 bbl/d followed by a 2-hr buildup. For this case $\Delta Z_R = 2.3$ ft and $25 r_w \sqrt{k_v / k_h} = 1.98$ ft, so the requirement of Eq. 13 is met. The pressure derivative and Horner plots for the buildup are presented in **Figs. 6** and **7**. The sink response in Fig. 6 has been included for reference only. The system reaches radial flow after 0.02 hours of buildup. Values for k_h and k_v are computed from the Horner straight line and they are shown in Fig. 7; k_h matches the input, whereas there is a slight error of 2.2% in the computed value of k_v.

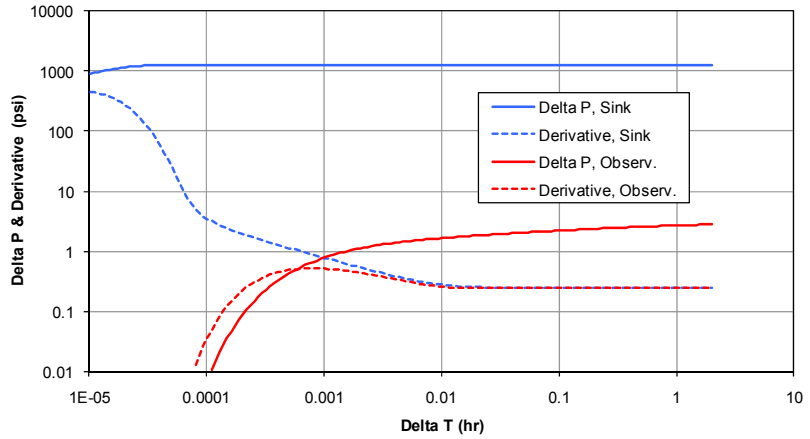

Fig.6—Pressure change and derivative for buildup, Case 1 (flowing through a single probe).

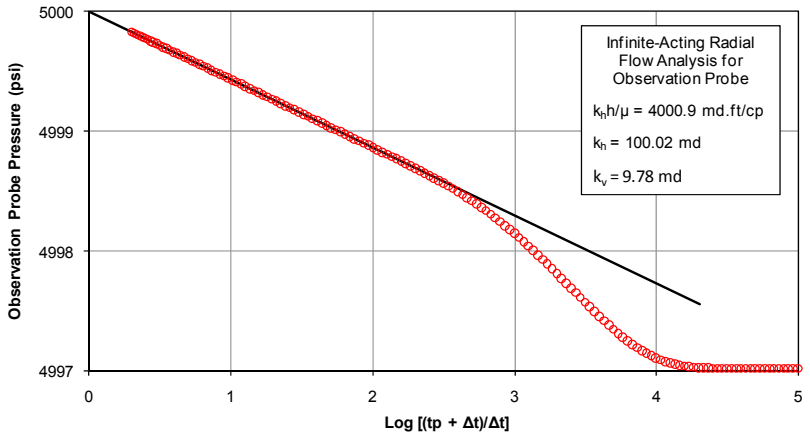

Fig.7—Horner analysis for buildup, Case 1 (flowing through a single probe).

Case 2. Dual-Packer Tool, with $k_h > k_v$. This case was generated using the same input as Case 1, except that the flowing probe was replaced by a dual packerwith$l_w = 1.6$ ft and the observation probe was placed at $z_o = 6.2$ ft. For this case $\Delta Z_R = 6.2$ ft

and $25\,r_w\sqrt{k_v/k_h} = 1.98$ ft, so the requirement of Eq. 13 is met. However, the length of the flowing interval is $2l_w = 3.2$ ft, which does not meet the requirement of being less than 0.62 ft (10% of ΔZ_R). The flowing-interval length exceeds 50% of ΔZ_R. The pressure derivative and Horner plots for the buildup are presented in **Figs. 8** and **9**. The dual-packer response in Fig. 8 has been included for reference only. The system reaches radial flow after 0.03 hours. The k_h and k_v values are computed from the Horner straight line and they are displayed in Fig. 9; k_h matches the input, whereas k_v is in error by 8.4%. This error is caused by the length of the flowing interval greatly exceeding the limit proposed by Prats of 10% of ΔZ_R. Nevertheless, an error of 8.4% in the computed k_v is considered acceptable for practical purposes.

Case 3. Single-Probe Tool, with $k_h < k_v$. This case was generated using the same input as Case 1, except the permeabilities were changed to $k_h = 25$ md and $k_v = 50$ md. For this case $\Delta Z_R = 2.3$ ft and $25\,r_w\sqrt{k_v/k_h} = 8.84$ ft, so the requirement of Eq. 13 is not met; even relaxing the 25 to 12 as proposed by Earlougher (1980) still fails Eq. 13 by a wide margin. The pressure derivative and Horner plots for the buildup are presented in **Figs. 10** and **11**. The system reaches radial flow after 0.005 hours. The k_h and k_v values are computed from the Horner straight line and they are shown in Fig. 11; k_h matches the input, whereas k_v is in error by 31%. This error is caused by failure to meet Prats' requirement of Eq. 13—with $k_h < k_v$ by a large amount, there is not enough separation between the probes when $z_o = 2.3$ ft.

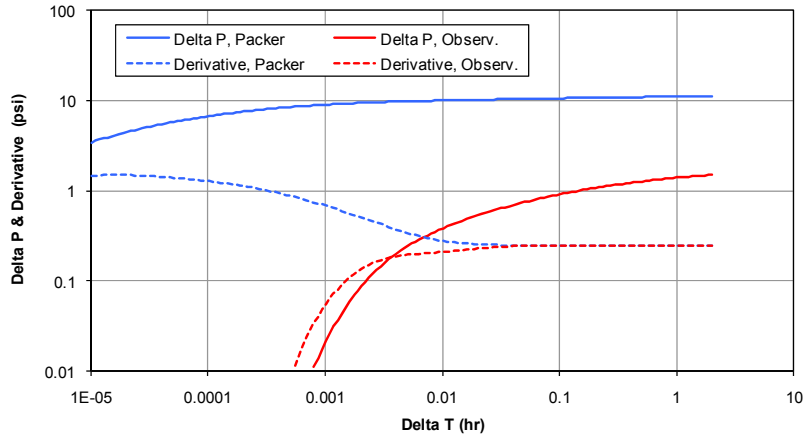

Fig.8—Pressure change and derivative for buildup, Case 2 (flowing through a dual packer).

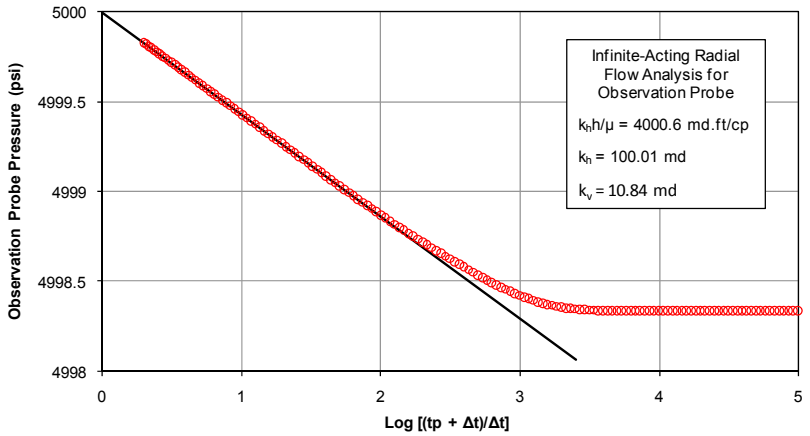

Fig.9—Horner analysis for buildup, Case 2 (flowing through a dual packer).

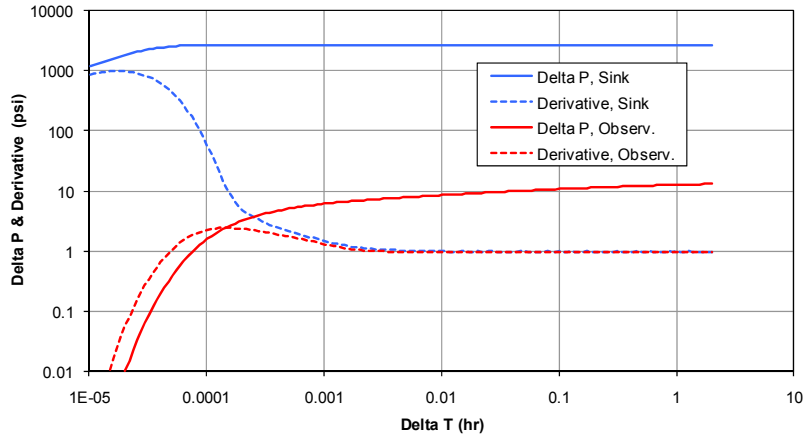

Fig.10—Pressure change and derivative for buildup, Case 3 (flowing through a single probe; z_o = 2.3 ft).

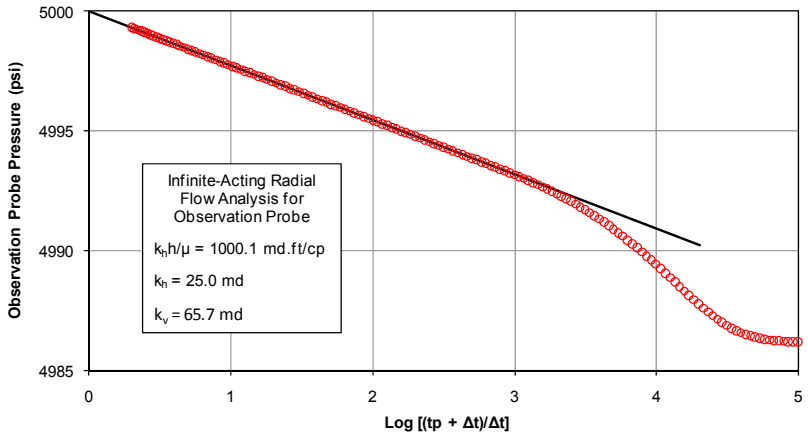

Fig.11—Horner analysis for buildup, Case 3 (flowing through a single probe; z_o = 2.3 ft).

To further examine this point, Case 3 was run again with $z_o = \Delta Z_R = 7.9$ ft. Such a value is representative of the probe spacing for a test conducted with two single-probe tools, as opposed to a dual-probe/single-probe combination, which is the basis for $z_o = 2.3$ ft. With $z_o = 7.9$ ft, the requirement of Eq. 13 is almost met (and it is easily met if 25 is relaxed to 12 as proposed by Earlougher). The derivative and Horner plots are shown in **Figs. 12** and **13**; Horner analysis now yields $k_v = 49.5$ md, which is just 1% in error.

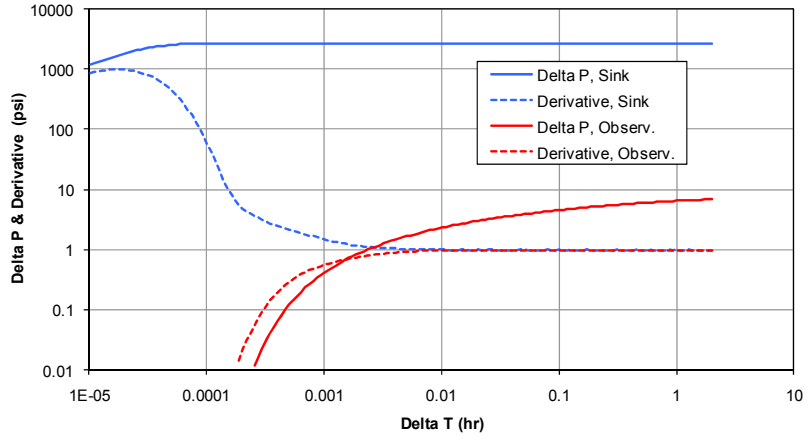

Fig.12—Pressure change and derivative for buildup, Case 3 (flowing through a single probe; z_o = 7.9 ft).

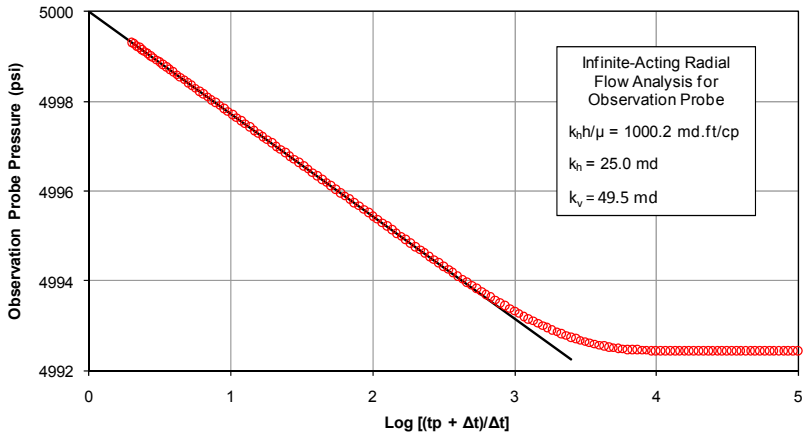

Fig.13—Horner analysis for buildup, Case 3 (flowing through a single probe; z_o = 7.9 ft).

Case 4. Dual-Packer Tool, with $k_h < k_v$. Case 4 was generated with the same input as Case 3, except that the flowing probe was replaced by a dual packer with $l_w = 1.6$ ft and the observation probe was placed at $z_o = 6.2$ ft. For this case $\Delta Z_R = 6.2$ ft and $25\, r_w \sqrt{k_v / k_h} = 8.84$ ft, so the requirement of Eq. 13 is not quite met (although it is met if 25 is relaxed to 12 as proposed by Earlougher, 1980). However, the length of the flowing interval is 3.2 ft, which does not meet the requirement of being less than 0.62 ft (10% of ΔZ_R). The flowing-interval length exceeds 50% of ΔZ_R. The pressure derivative and Horner plots for the buildup are displayed in **Figs. 14** and **15**. The system reaches radial flow after 0.005 hours. Horner analysis results for k_h and k_v are shown in Fig. 15. The k_h value matches the input; however, k_v is in error by 8.2%. The magnitude of the error is similar to that seen in Case 2, suggesting that it is caused by the length of the flowing interval greatly exceeding the limit proposed by Prats. It does not appear as if the slight error in meeting the requirement of Eq. 13 has had an effect on the error in k_v.

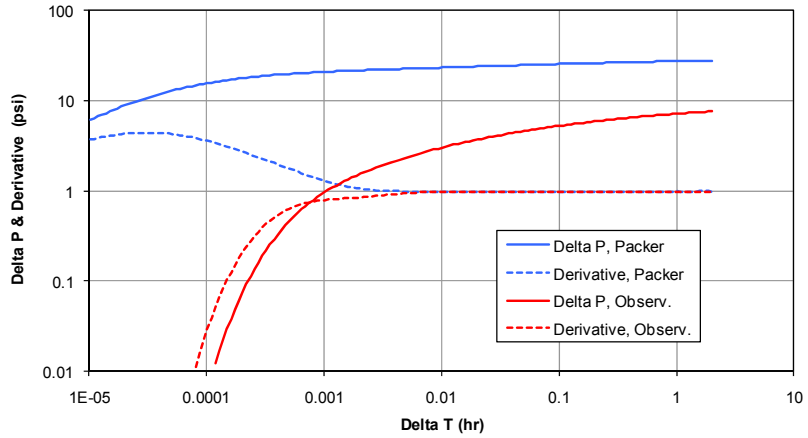

Fig.14—Pressure change and derivative for buildup, Case 4 (flowing through a dual packer).

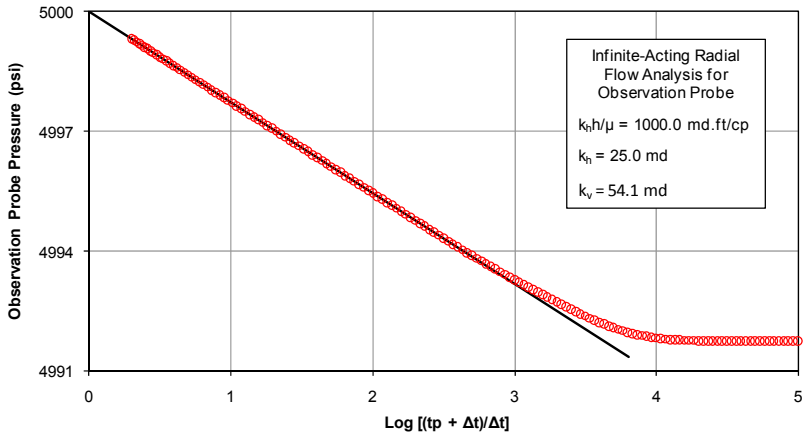

Fig.15—Horner analysis for buildup, Case 4 (flowing through a dual packer).

Extension of Prats' Method to Inclined Wellbores and 3D Permeability Anisotropy

Prats developed his method for vertical wells with 2D permeability anisotropy. Here we extend the method to the general case of an inclined wellbore in a reservoir with 3D permeability anisotropy. The wellbore inclination, θ_w, (see Fig. 3) can range from 0° (vertical) to 90° (horizontal). As detailed in Appendix B, we can use the transformations, based on the work of Besson (1990), to adapt Eq. 1 for wellbore inclination and 3D anisotropy. The adapted equations for all inclination angles of the wellbore and 3D anisotropic medium are given in Appendix B.

To evaluate our extension of Prats' method to inclined wellbores, here for simplicity, we consider only the case of a 2D anisotropic medium and check the validity of Eqs. 1, 2, and B-15–B-17 by using the analytical solution of Abbaszadeh and Hegeman (1990). We compare the intercept of the radial-flow plot, b, given by Eqs. B-15–B-17 with that from radial-flow analysis of data from the Abbaszadeh and Hegeman solution. For a 2D anisotropic medium, $\eta=1$; therefore Eq. B-15 can be written as

$$b = 162.6\frac{q\mu}{k_h h}\left[\frac{\tilde{G}^* + \dfrac{h}{\sqrt{\cos^2\theta_w + (k_v/k_h)\sin^2\theta_w}\,|z_o|}}{2.303} + \log\left(\frac{0.0002637k_v}{\phi\mu c_t h^2}\right)\right]. \quad \text{..... (14)}$$

$\tilde{G}^*$ is given by Eq. B-16 with $\tilde{Z} = \left(z_w + \sqrt{\cos^2\theta_w + (k_v/k_h)\sin^2\theta_w}\; z_o\right)/h$, and $\tilde{Z}' = z_w/h$.

The restriction on z_o given by Eq. B-21 for a 2D anisotropic medium can be written as

$$|z_o| > \frac{12.5\, r_w\sqrt{k_v/k_h}}{\sqrt{\cos^2\theta_w + (k_v/k_h)\sin^2\theta_w}}\left(1 + \frac{1}{\sqrt{\cos^2\theta_w + (k_v/k_h)\sin^2\theta_w}}\right). \quad \text{..... (15)}$$

Eqs. 14 and 15 apply for all values of well inclination, $0° \le \theta_w \le 90°$ for a 2D anisotropic medium.

Table 1 compares the values of b computed from Eq. 14 and from the Abbaszadeh and Hegeman solution for a case where the anisotropy ratio $k_v/k_h = 0.1$, as a function of the inclination angle of the well for a case of constant-rate flow at 14 bbl/d. The test duration was long enough so that the observation-probe pressure exhibited a well-defined radial-flow regime. Table 1 also presents the values of the z_o requirement computed from the right-hand side of Eq. 15. Other input parameter values were taken from Case 2 presented previously: $h = 20$ ft, $k_h = 100$ md, $k_v = 10$ md, $z_w = 8$ ft, $z_o = 6.2$ ft, $\mu = 0.5$ cp, $\phi = 0.2$, $c_t = 8\times10^{-6}$ 1/psi, $p_{i,o} = 5000$ psi, $l_w = 1.6$ ft, and $r_w = 0.25$ ft.As is seen from Table 1, the error in the value of b from Eq. 14 for this value of anisotropy ratio for all inclination angles is less than 2% when compared with the corresponding value obtained from the Abbaszadeh and Hegeman solution. We note that $z_o = 6.2$ ft for this case, so only inclination angles less than 80° of Table 1 meet the requirement given by Eq. 15; however, the error in b is largely unaffected by this.

TABLE 1—COMPARISON OF *b* FROM EQ. 14 AND FROM ABBASZADEH AND HEGEMAN (1990) ANALYTICAL SOLUTION FOR AN INCLINED WELL WITH 2D PERMEABILITY ANISOTROPY ($k_v/k_h=0.1$).

Inclination angle θ_w, degrees	*b*, psi Eq. 14	*b*, psi Abbaszadeh and Hegeman	% error in *b* from Eq. 14	z_o requirement, ft Eq. 15
0 (vertical)	1.475	1.494	1.31	1.98
15	1.498	1.518	1.29	2.07
30	1.578	1.598	1.27	2.40
45	1.743	1.766	1.30	3.13
65	2.228	2.261	1.48	5.73
80	2.905	2.954	1.66	10.54
90 (horizontal)	3.191	3.251	1.84	13.01

Table 2 presents a comparison for the case of anisotropy ratio $k_v/k_h = 2.0$. Like the previous case, we consider a drawdown test of constant-rate flow at 14 bbl/d for sufficiently long duration so that the observation-probe pressure exhibited a well-defined radial-flow regime. Table 2 also presents the values of the z_o requirement computed from the right-hand side of Eq. 15. Other input parameter values were taken from Case 4 presented previously: $h = 20$ ft, $k_h = 25$ md, $k_v = 50$ md, $z_w = 8$ ft, $z_o = 6.2$ ft, $\mu = 0.5$ cp, $\phi = 0.2$, $c_t = 8\times10^{-6}$1/psi, $p_{i,o} = 5000$ psi, $l_w = 1.6$ ft, and $r_w = 0.25$ ft.As is seen from Table 2, the error in the value of *b* from Eq. 14 for this value of anisotropy ratio for all inclination angles is less than 5% when compared with the corresponding value obtained from the Abbaszadeh and Hegeman solution. We note that $z_o = 6.2$ ft for this case, so inclination angles greater than 45° of Table 2 meet the requirement given by Eq. 15; however, like in the previous case, the error in *b* is largely unaffected by this.Thus, from the results of Tables 1 and 2, we conclude that Eq. 14 provides a good approximation for the radial-flow plot intercept and hence for the vertical permeability to be computed from this intercept.

TABLE 2—COMPARISON OF *b* FROM EQ. 14 AND FROM ABBASZADEH AND HEGEMAN (1990) ANALYTICAL SOLUTION FOR AN INCLINED WELL WITH 2D PERMEABILITY ANISOTROPY ($k_v/k_h=2.0$).

Inclination angle θ_w, degrees	*b*, psi Eq. 14	*b*, psi Abbaszadeh and Hegeman	% error in *b* from Eq. 14	z_o requirement, ft Eq. 15
0 (vertical)	7.490	7.568	1.03	8.84
15	7.395	7.431	0.48	8.42
30	7.181	7.133	0.67	7.49
45	6.964	6.810	2.26	6.55
65	6.767	6.496	4.17	5.70
80	6.699	6.392	4.80	5.39
90 (horizontal)	6.686	6.398	4.50	5.33

Analysis Procedure for Inclined Wellbores and 3DPermeability Anisotropy

As mentioned previously, Prats' method as described by Eqs. 1–5 is valid for a vertical well in a 2D anisotropic medium. As we have shown in Appendix B, for inclined wells and 3D anisotropy, Eqs. 1, 2, and B-15–B-17 apply. Also, we have shown that for a vertical well in a 3D anisotropic medium, $\delta = 1$ and thus Eqs. B-15–B-17 are identical to Eqs. 3–5; therefore, Prats' method applies for all vertical wells, regardless of the degree of anisotropy.

For inclined wells, application of Prats' method of Eqs. 1–5 will result in significant error in the analysis. To demonstrate this, the Abbaszadeh and Hegeman solution data from the example of Table 1 have been analyzed assuming the well to be vertical. The results show that for all cases k_h is correctly determined to be 100 md. Table 3 lists the computed k_v values; the correct value of k_v is 10 md. Note that the error of 8.4% at 0° inclination is the inherent error in Prats' method as shown earlier for Case 2. In summary, these results indicate that Prats'vertical-well method can be applied for wellbore inclinations up to about 15° without introducing significant error; however, for larger inclinations, the error in k_v becomes unacceptable.

For inclined wells, the intercept *b* given by Eq. B-15 is a nonlinear function of k_v, k_h, θ_w, and η for the case of 3D anisotropy. For a 2D anisotropic medium, $\eta=1$; thus the intercept *b* is a nonlinear function of k_v, k_h, and θ_w, as given by Eq. 14. For a test conducted in an inclined well, radial-flow analysis will provide values for k_h and *b*. Therefore, to obtain a value for k_v, a nonlinear solution technique must be used. In addition, values for θ_w and η (if 3D) must be knowna priori. The inclination and azimuth angles of the well (θ_w and θ', respectively) are usually known from a drilling survey. For the case of 3D

anisotropy, an estimate for k_x/k_y can usually be obtained from core data or geologic modeling; values for k_x/k_y and θ' are required to estimate η.

TABLE 3—COMPUTED k_v (ASSUMING A VERTICAL WELL) FOR AN INCLINED WELL WITH 2D PERMEABILITY ANISOTROPY ($k_v/k_h=0.1$)

Inclination angle θ_w, degrees	k_v, md	% error in k_v
0 (vertical)	10.84	8.4
15	11.93	19.3
30	16.5	65
45	32.6	226
65	242	2,320
80	3,980	39,700
90 (horizontal)	13,270	132,600

To further illustrate the analysis procedure for determining k_v for an inclined well, we consider the case of 2D anisotropy. We are required to find a value of k_v that satisfies Eq. 14 for the values of for k_h and b from radial-flow analysis, and the given values of well and reservoir parameters such as θ_w, h, μ, z_o, z_w, q, ϕ, r_w, and c_t. This requirement can be expressed as

$$f(k_v) = b - 162.6\frac{q\mu}{k_h h}\left[\frac{\tilde{G}^* + \dfrac{h}{\sqrt{\cos^2\theta_w + (k_v/k_h)\sin^2\theta_w}\,|z_o|}}{2.303} + \log\left(\frac{0.0002637k_v}{\phi\mu c_t h^2}\right)\right] = 0 \quad \text{..... (16)}$$

Note that $\tilde{G}^*$ is also a function of k_v. Eq. 16 is a nonlinear function of k_v. The Newton-Raphson method (Press et al. 2007) is suitable for solving this nonlinear equation for k_v. This method requires the derivative of the function, which requires the derivative of $\tilde{G}^*$; this in turn requires the derivative of the digamma function, Ψ. Amos (1983) presents an algorithm for this derivative.

An alternative to a nonlinear solution technique is a graphical technique. This involves plotting $f(k_v)$ vs. k_v, and visually finding the zero point. As an example, the data used to generate Table 1 have been used with Eq. 16 to compute $f(k_v)$ vs. k_v, for the case of $\theta_w=45°$, and the result is displayed in **Fig. 16**. It can be seen from the figure that $f(k_v)=0$ at $k_v=10$ md, which is the correct solution.

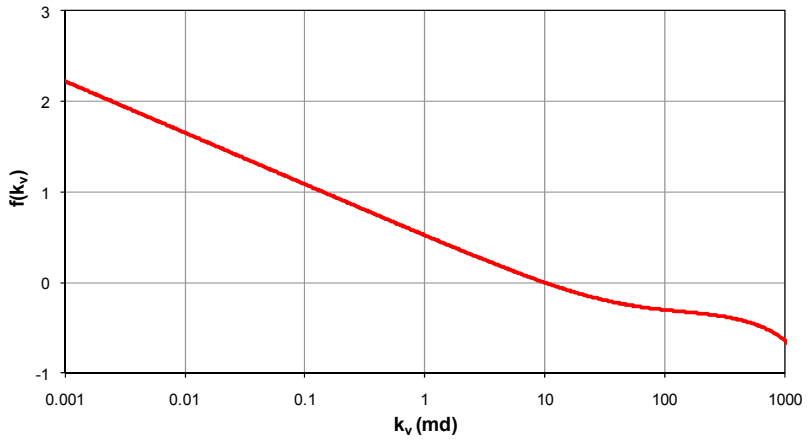

Fig. 16—$f(k_v)$ vs. k_v for $\theta_w=45°$.

Field Example Application

This example is for an IPTT conducted in a vertical well. The tool used was a dual-packer module with a vertical observation probe mounted 6.4 ft above the packer in an 11-ft-thick water zone (**Fig. 17**). The other pertinent parameters are $z_w=2$ ft, $l_w=1.6$ ft, $z_o=6.4$ ft, $c_t=8\times10^{-6}$1/psi, $r_w=0.354$ ft, $C_w=2.0\times10^{-6}$bbl/psi, $\mu=1$ cp, and $\phi=0.22$. The test consisted of a 0.5-hr

pumpout period, during which about 34 L of water was produced, followed by 1-hr buildup. The average flow rate before buildup is 10 bbl/d.

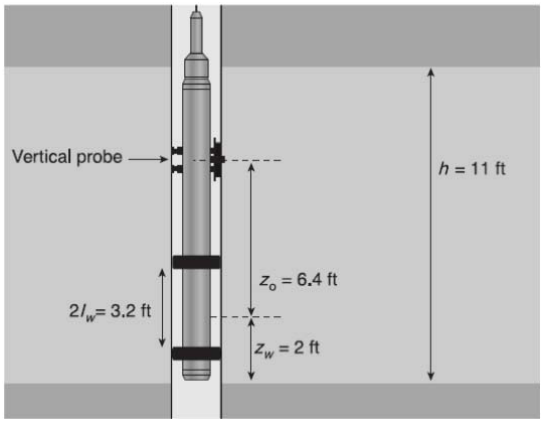

Fig. 17—Schematic diagram of the tool configuration for the field IPTT test.

The buildup pressure derivative for the packer and probe are shown in **Fig. 18**; these data identify the flow regimes that occurred during the test.The derivative data at both locations show that radial flow is established at about 0.15 hours. In the time interval from 0.014 to 0.1hours the dual-packer derivative shows a well-defined –1/2 slope line, indicating either spherical or hemispherical flow. For the given values of h, z_w, and l_w, the dual-packer interval is so close to the bottom of the zone that we would expect the response to go almost immediately to hemispherical flow, without any discernible transition from spherical to hemispherical. So, the –1/2 slope observed in packer-derivative should be that of the hemispherical flow. Overall the derivative signature is typical of a single-layer formation with sealed top and bottom boundaries, and this is consistent with geological and log data.

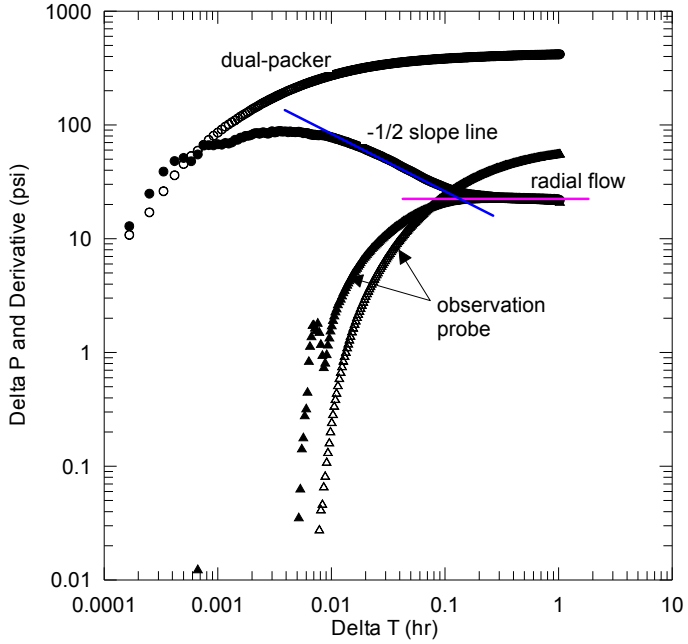

Fig. 18—Buildup pressure change and derivative at the packer interval and observation probe, field example.

Fig. 19 presents the radial-flow analysis for the observation probe. The k_h value of 2.82 md is computed from the straight-line slope; the k_v value of 2.52 md is computed with Prats' method. For this case $z_o = 6.4$ ft; this value does not exceed $25 r_w \sqrt{k_v / k_h} = 8.3$ ft, so the requirement of Prats is not met. Note that if we replace the constant 25 by 12 as suggested by Earlougher (1980), then the requirement is met. The length of the flowing interval is $2l_w = 3.2$ ft, which does not meet the requirement of being less than 0.64 ft (10% of z_o). However, in the synthetic examples that were examined, this never introduced appreciable error. From the radial-flow analysis a value of spherical permeability can be estimated as $k_s = (k_h^2 k_v)^{1/3} = (2.82^2 \times 2.52)^{1/3} = 2.72$ md. The observation probe does not exhibit spherical flow for this test; therefore, we

cannot perform the spherical-flow analysis method of Onur et al. (2011) to estimate the individual values of k_h and k_v as well as the spherical permeability k_s, and check this value with that computed from the radial-flow analysis. However, the dual-packer data exhibit a well-defined hemispherical flow in the time interval from 0.014 to 0.1 hours, so we can perform a hemispherical-flow analysis of the dual-packer data. This analysis yields $k_s = 2.47$ md (**Fig. 20**), which is in good agreement with the 2.72-md value estimated from radial-flow analysis of the observation-probe data.

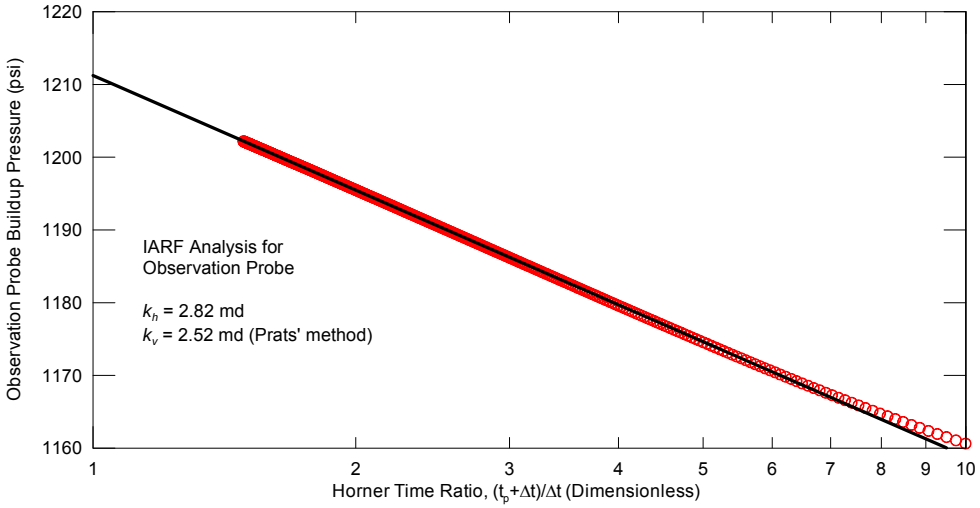

Fig. 19—Radial-flow analysis for buildup at the observation probe, field example.

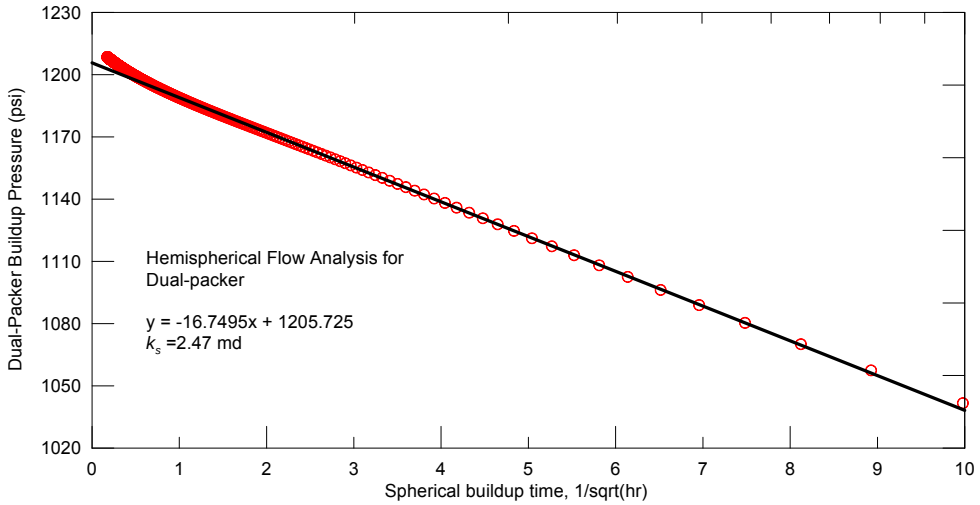

Fig.20—Hemispherical-flow analysis for buildup at the dual packer, field example.

Fig. 21 presents model-generated pressure change and derivative for the observation probe using the radial-flow results of $k_h = 2.82$ md and $k_v = 2.52$ md. **Figs. 22**and **23** display the simulated observation-probe and dual-packer pressures over the entire test interval, respectively. To generate the simulated responses shown in Fig. 22, we used a mechanical skin factor of $S = 0.41$, which was estimated from nonlinear regression analysis by Onur et al. (2004). The matches shown in Figs. 21–23 are good. These k_h and k_v values are also quite close to those determinedby Onur et al. (2004); they used nonlinear regression analysis based on pressure-pressure convolution to obtain $k_h = 2.81$ md, $k_v = 2.58$ md, and $S = 0.41$. In summary, application of Prats' method to the observation-probe buildup data of this vertical-well IPTT provides values of horizontal and vertical permeability. These values provide good matches of the observation-probe pressures and the dual-packer pressures.

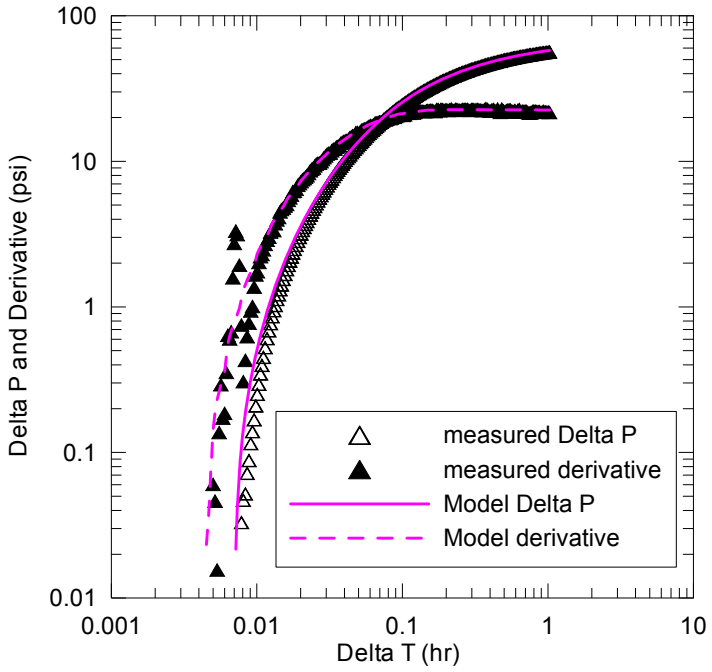

Fig.21—Model pressure change and derivative for observation-probe buildup using results from radial-flow analysis.

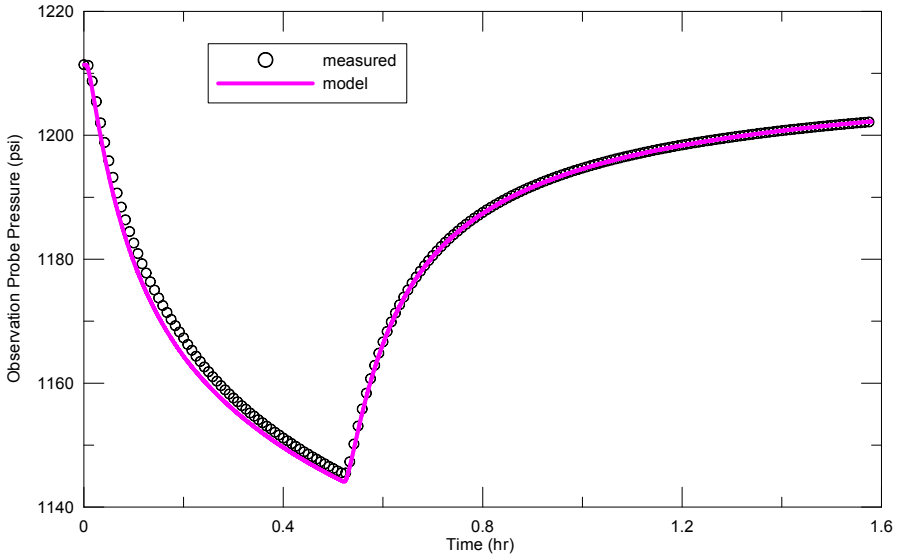

Fig.22—Simulated pressure for observation probe using k_h = 2.82 md and k_v = 2.52 md from radial-flow analysis.

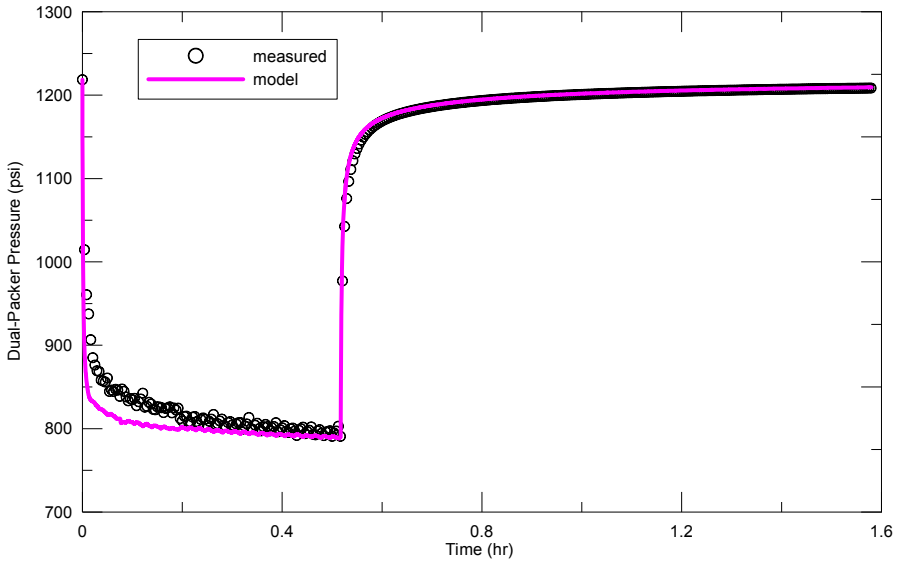

Fig.23—Simulated pressure for dual packerusing k_h=2.82 md and k_v=2.52 md from radial-flow analysis.

Conclusions

We have presented a method to determine the horizontal and vertical permeability from the radial-flow response at an observation probe of an IPTT. The method applies for tests conducted with a single-probe or dual-packer module. The method is based on an adaptation of a well-testing method presented by Prats (1970) for vertical wells with 2D permeability anisotropy. We have extended the method to the general case of an inclined wellbore in a reservoir with 3D permeability anisotropy. The wellbore inclination can range from 0° (vertical) to 90° (horizontal). Furthermore, Prats developed his method for the case of producing (injecting) the well at a constant flow rate. However, in practice, it can be difficult to maintain a constant rate; thus, we have adapted the method for the case where the production period is followed by a buildup test.

We have used our extension of Prats' method to analyze pressure data acquired at an IPTT observation probe; synthetic cases and a field dual-packer IPTT test have been evaluated. The analysis results for the synthetic cases are generally in good agreement with the input values. For the field test, the value of k_v obtained from our radial-flow analysis agrees well with resultsobtained from spherical-flow analysis and nonlinear regression analysis. In cases where Prats' requirements are violated, error is seen in the k_v result; k_h is always determined without error. For IPTT tests conducted where k_v exceeds k_h by a factor of two or more, the observation-probe spacing may be designed so that analysis requirements are not violated. For dual-packer IPTT tests where analysis requirements on the length of the flowing interval are exceeded by a large margin, the synthetic cases and the field test show that the error in k_v remains less than 10%, which is acceptable.

Nomenclature

$a_1 - a_4$ = constants used in the digamma function
a_x = constant defined by Eq. B-10, dimensionless
a_y = constant defined by Eq. B-11, dimensionless
a_z = constant defined by Eq. B-12, dimensionless
b = intercept of radial-flow plot, m/Lt^2, psi
c_t = total compressibility, Lt^2/m, 1/psi
C_w = wellbore or tool storage constant at the dual-packer location, L^{4}t^2/m, bbl/psi
f = nonlinear function defined by Eq. 16
G^* = geometrical function, dimensionless
h = formation thickness, L, ft
k_h = horizontal permeability, L^2, md
k_s = spherical permeability, L^2, md
k_v = vertical permeability,L^2, md
k_x = horizontal permeability in x-direction of a 3D anisotropic formation,L^2, md
k_y = horizontal permeability in y-direction of a 3D anisotropic formation,L^2, md
k_z = vertical permeability (in z-direction) of a 3D anisotropic formation,L^2, md
l_w = half-length of the open interval, L, ft
log = logarithm based 10
m = slope of radial-flow plot (absolute value), m/Lt^2, psi
m_{sp} = slope of straight line on a spherical-flow plot,m/Lt$^{3/2}$, psi-hour$^{1/2}$

$p_{i,o}$ = initial formation pressure at the observation point, m/Lt^2, psi
$p_{wf,o}$ = flowing pressure at the observation point, m/Lt^2, psi
$p_{ws,o}$ = buildup pressure at the observation point, m/Lt^2, psi
q = flow rate, L^3/t, bbl/d
r_p = probe radius, L, inches
r_w = wellbore radius, L, ft
S = mechanical skin factor, dimensionless
t = time, t, hour
t_p = producing time, t, hour
x = x coordinate in Cartesian coordinate system, L, ft
y = y coordinate in Cartesian coordinate system, L, ft
z = z coordinate in Cartesian and cylindrical coordinate systems, L, ft
Z = location of observation perforation, dimensionless
Z' = location of producing perforation, dimensionless
z_o = measured distance from the center of the producing probe/packer to observation probe, L, ft
z_w = vertical distance from the bottom of the formation to the center of the producing probe/packer, L, ft
α = constant defined by Eq. 8, dimensionless
β = constant defined by Eq. 12, dimensionless
δ = constant defined by Eq. B-14, dimensionless
γ = Euler's constant, equal to 0.57721…
Δt = elapsed (or shut-in) time during buildup, t, hour
ΔZ_P = distance from the producing perforation to the top of the formation, L, ft
ΔZ_R = distance from the observation perforation to the producing perforation, L, ft
ΔZ_{wf} = distance from the bottom of the formation to the producing perforation, L, ft
ΔZ_{ws} = distance from the bottom of the formation to the observation perforation, L, ft
η = constant defined by Eq. B-13, dimensionless
θ' = azimuth angle of the well from x-axis, degrees
θ_w = inclination angle of well, degrees [0 (vertical) to 90 (horizontal)]
μ = viscosity, m/Lt, cp
ϕ = porosity, fraction
Ψ = digamma function (i.e., logarithmic derivative of the gamma function)

Subscripts

h = horizontal
i = initial or index
o = observation probe
p = coordinate of probe
t = total
v= vertical
w = well or wellbore
x= x-direction
y = y-direction
z = z-direction

Superscripts

$\bar{}$ = effective properties in an equivalent isotropic medium
$\sim$= effective property in a 3D anisotropic medium

Acknowledgement

We thank Universiti Teknologi PETRONAS and Schlumberger for permission to present this paper. The first author also wishes to acknowledge the support provided by the Research & Innovation Office and the Petroleum Engineering Department at Universiti Teknologi PETRONAS.

References

Abbaszadeh, M. and Hegeman, P.S. 1990. Pressure-Transient Analysis for a Slanted Well in a Reservoir with Vertical Pressure Support.*SPEForm Eval***5** (3): 277–284.SPE-19045-PA. DOI: 10.2118/19045-PA.

Amos, D.E. 1983. A Portable FORTRANSubroutine for Derivatives of the Psi Function, Algorithm 610, *ACM Transactions on Mathematical Software* **9** (4): 494–502.

Besson, J. 1990. Performance of Slanted and Horizontal Wells on an Anisotropic Medium. Paper SPE 20965 presented at the EUROPEC 90, The Hague, Netherlands, 22–24 October. DOI: 10.2118/20965-MS.

Carter, R.D., Kemp, L.F. Jr., Pierce, A.C., and Williams, D.L. 1974. Performance Matching with Constraints. *SPE J* **14**(2): 187–196. SPE-4260-PA.DOI: 10.2118/4260-PA.

Cody, W., Strecok, A., and Thacher, H. 1973. Chebyshev Approximations for the Psi Function. *Mathematics of Computation* **27**(121): 123–127.

Earlougher, R.C. Jr. 1977.*Advances in Well Test Analysis*, Monograph Series No. 5, SPE, Dallas, TX (1977).

Earlougher, R.C. Jr. 1980. Analysis and Design Methods for Vertical Well Testing. *J Pet Technol* **32** (3): 505–514. SPE-8038-PA. DOI: 10.2118/8038-PA.

Goode, P.A., and Thambynayagam, R.K.M. 1992. Permeability Determination with a Multiple Probe Formation Tester. *SPE Form Eval*, **7** (4): 297–303. SPE-20737-PA. DOI: 10.2118/20737-PA.

Kuchuk, F.J. 1994. Pressure Behavior of the MDT Packer Module and DST in Crossflow-Multilayer Reservoirs.*J. Pet Sci. Eng.* **11** (2): 123–135.

Kuchuk, F.J., Ramakrishnan, T.S., and Dave, Y. 1994. Interpretation of Wireline Formation Tester Packer and Probe Pressures. Paper SPE 28404 presented at the SPE Annual Technical Conference and Exhibition, New Orleans, LA, 25–28 September. DOI: 10.2118/28404-MS.

Kuchuk, F.J. 1996. Multiprobe Wireline Formation Tester Pressure Behavior in Crossflow-Layered Reservoirs. *InSitu* **20**(1): 1–40.

McKinley, R.M., Vela, S., and Carlton, L.A.1968. A Field Application of Pulse-Testing for Detailed Reservoir Description. *J Pet Technol* **20** (3): 313–321. SPE-1822-PA.DOI: 10.2118/1822-PA.

Onur, M.**,** Hegeman, P.S., and Kuchuk, F.J. 2004. Pressure/Pressure Convolution Analysis of Multiprobe and Packer-Probe Wireline Formation Tester Data.*SPE Res Eval&Eng* **7**(5): 351–364. SPE-77343-PA. DOI: 10.2118/77343-PA.

Onur, M., Çınar, M., Ilk, D., Valko, P.P., Blasingame, T.A. and Hegeman, P.S. 2008. An Investigation of Recent Deconvolution Methods for Well-Test Data Analysis. *SPE J.* **13**(2): 226–247. SPE-102575-PA. DOI: 10.2118/102575-PA.

Onur, M, Hegeman, P.S., Gok, I.M, and Kuchuk, F.J.2011. A Novel Analysis Procedure for Estimating Thickness-Independent Horizontal and Vertical Permeabilities from Pressure Data at an Observation Probe Acquired by Packer-Probe Wireline Formation Testers.*SPERes Eval&Eng* **14**(4): 457–472. SPE-148403-PA. DOI: 10.2118/148403-PA.

Pimonov, E., Ayan, C., Onur, M., and Kuchuk, F.J. 2010. New Pressure/Rate Deconvolution Algorithm to Analyze Wireline Formation Tester and Well-Test Data. *SPERes Eval&Eng* **13**(4): 603–613. SPE-123982-PA. DOI: 10.2118/123982-PA.

Pop, J.J., Badry, R.A., Morris, C.V., Wilkinson, D.J., Tottrup, P., and Jonas, J.K. 1993. Vertical Interference Testing with a Wireline Conveyed Straddle Packer Tool.Paper SPE 26841 presented at the SPE Annual Technical Conference and Exhibition, Houston, TX, 3–6 October. DOI: 10.2118/26841-MS.

Press, W.H., Flannery, B.P., Teukolsky, A.A., and Vetterling, W.T. 2007. *Numerical Recipes: The Art of Scientific Computing*, Cambridge University Press, ISBN 0-521-88068-8.

Prats, M. 1970. A Method for Determining the Net Vertical Permeability Near a Well From In-Situ Measurements*. J. Pet Tech* **22** (5): 637–643. SPE-2511-PA.DOI: 10.2118/2511-PA.

von Schroeter, T., Hollaender, F., and Gringarten, A.C. 2004. Deconvolution of Well Test Data as a Nonlinear Total Least-Squares Problem. *SPE J* **9**(4): 375–390. SPE-77688-PA. DOI: 10.2118/77688-PA.

Zimmerman, T., McInnis, J.,Hoppe, J., Pop, J.J., and Long, T. 1990. Application of Emerging Wireline Formation Technologies. Paper OSEA 90105 presented at the Offshore South East Asia Conference, Singapore, 4–7 December.

Appendix A—Terminology

The terms "horizontal permeability" and "vertical permeability" are commonly used to refer to permeability values parallel to the formation bed boundaries and perpendicular to the formation bed boundaries, respectively. However, if the formation bed boundaries are not actually horizontal, then horizontal permeability and vertical permeability will not actually be horizontal and vertical, respectively. Nevertheless, the terms horizontal permeability and vertical permeability are used to refer to permeability parallel to the bed boundaries and perpendicular to the bed boundaries, respectively, throughout this paper. In a similar manner as "horizontal" and "vertical" permeability, a "vertical well" is considered to be a wellbore drilled perpendicular to the formation bed boundaries, whereas a "horizontal well" is considered to be a wellbore drilled parallel to the formation bed boundaries. Thus, if the formation bed boundaries are not actually horizontal, then a vertical well and a horizontal well will not actually be vertical and horizontal, respectively.

The term "anisotropy" refers to the variation of a property with the direction in which it is measured. Rock permeability is a measure of its conductivity to fluid flow through its pore spaces. Reservoir rocks often exhibit permeability anisotropy—conductivity to fluid depends on the direction of flow. This is most often true when comparing permeability measured parallel to bed boundaries ("horizontal permeability," k_h) and permeability measured perpendicular to bed boundaries ("vertical permeability," k_v). Such permeability anisotropy is referred to as 2D anisotropy. In some cases, there may even be anisotropy within the plane parallel to bed boundaries, such that instead of a single value of horizontal permeability (k_h), there are separate components measured in orthogonal directions, referred to as k_x and k_y. A rock that exhibits variation in permeability when measured vertically as well as both horizontal directions is said to have 3D anisotropy. A rock that exhibits no directional variation in permeability is referred to as "isotropic."

Appendix B—Derivation of Radial-Flow Equation for an Observation Probe for Inclined Wellbores and 3D Permeability Anisotropy

Here, we extend the Prats' (1970) method to the general case by deriving radial-flow equation for an observation probe positioned along an inclined wellbore in a reservoir with 3D permeability anisotropy. The wellbore inclination, θ_w, can range from 0° (vertical) to 90° (horizontal). Our starting point is the infinite-acting radial-flow equation for the observation probe in

an isotropic medium (i.e.,$k_h = k_v = k$) of finite thickness h. This equation (for a constant-rate drawdown test) is given by Eq. 1 where k_h and k_v are replaced by k. Then, the following transformations, based on the work of Besson (1990), can be used to adapt Eq. 1 with $\bar{k} = k_h = k_v$ for an equivalent isotropic system for wellbore inclination and 3D anisotropy:

$$\bar{k} = k_s = \sqrt[3]{k_h^2\, k_v}\,, \quad \text{(B-1)}$$

$$\bar{x} = a_x\, x\,, \quad \text{(B-2)}$$

$$\bar{y} = a_y\, y\,, \quad \text{(B-3)}$$

$$\bar{z} = a_z\, z\,, \quad \text{(B-4)}$$

$$\bar{h} = a_z\, h\,, \quad \text{(B-5)}$$

$$\overline{l_w} = a_z\, \delta\, l_w\,, \quad \text{(B-6)}$$

$$\overline{z_o} = a_z\, \delta\, z_o\,, \quad \text{(B-7)}$$

$$\tan\overline{\theta'} = \sqrt{k_x / k_y}\, \tan\theta'\,, \quad \text{(B-8)}$$

and

$$\tan\overline{\theta_w} = (\eta/\delta)\, \tan\theta_w\,. \quad \text{(B-9)}$$

The parameters a_x, a_y, a_z, η, and δ in Eqs. B-1–B-8 are defined as, respectively,

$$a_x = \sqrt[6]{k_v / k_h}\ \sqrt[4]{k_y / k_x}\,, \quad \text{(B-10)}$$

$$a_y = \sqrt[6]{k_v / k_h}\ \sqrt[4]{k_x / k_y}\,, \quad \text{(B-11)}$$

$$a_z = \sqrt[3]{k_h / k_v}\,, \quad \text{(B-12)}$$

$$\eta = \sqrt{\sqrt{k_y / k_x}\cos^2\theta' + \sqrt{k_x / k_y}\sin^2\theta'}\,, \quad \text{(B-13)}$$

and

$$\delta = \sqrt{\cos^2\theta_w + (k_v / k_h)\,\eta^2 \sin^2\theta_w}\,. \quad \text{(B-14)}$$

In Eqs. B-1–B-14, k_h represents the geometric permeability on the horizontal plane, i.e., $k_h = \sqrt{k_x k_y}$, and k_v ($=k_z$) represents the vertical permeability.Also, we use the terminology of Figs. 1–3: $z_w = \Delta Z_{wf}$ and $z_o = \Delta Z_R$.

Using Eq. B-1 for transforming k, Eq. B-4 for z_w, Eq. B-5 for h, and Eq. B-7 for z_o, we obtain the radial-flow equation for an observation probe in a 3D anisotropic porous medium for all inclination angles of a well. The result is that Eqs. 1 and 2 in the main text remain unchanged; however, the intercept of the radial-flow plot, b, becomes

$$b = 162.6\frac{q\mu}{k_h h}\left[\frac{\widetilde{G}^* + \dfrac{h}{\delta\,|z_o|}}{2.303} + \log\left(\frac{0.0002637 k_v}{\phi\mu c_t h^2}\right)\right]. \quad \text{(B-15)}$$

$\widetilde{G}^*$ is given by

$$\widetilde{G}^* = \frac{1}{\widetilde{Z} + \widetilde{Z}'} - 2\ln 2 - \gamma - \frac{1}{2}\sum_{i=1}^{4}\Psi\left(\frac{\widetilde{a}_i + 1}{2}\right) \quad \text{(B-16)}$$

where $\widetilde{Z} = (z_w + \delta\, z_o)/h$, $\widetilde{Z}' = z_w / h$, and

$$\widetilde{a}_1 = 1 + \widetilde{Z} + \widetilde{Z}'\,;\ \widetilde{a}_2 = 1 + \widetilde{Z} - \widetilde{Z}'\,;\ \widetilde{a}_3 = 1 - \widetilde{Z} + \widetilde{Z}'\,;\ \widetilde{a}_4 = 1 - \widetilde{Z} - \widetilde{Z}'\,. \quad \text{(B-17)}$$

Note that for a 2D anisotropic medium, where we assume permeability is isotropic in the horizontal plane (i.e., $k_x = k_y$), we obtain $\eta = 1$ from Eq. B-13.

As noted earlier in the section "Discussion and Limitations of Prats' Method," the method is based on the assumption of a zero-radius (i.e., line-source) wellbore. For Eqs. 1–5 to apply to a finite-radius wellbore in an isotropic medium (i.e., $k_h = k_v$), Eq. 13 becomes

$$|z_o| > 25 r_w\,. \quad \text{(B-18)}$$

Therefore, for Eqs. 1, 2, and B-15–B-17 to apply to a finite-radius inclined wellbore in a reservoir with 3D permeability anisotropy, Eq. B-18 must be transformed. We use Eq. B-7 to replace z_o; r_w is replaced by the expression given by Besson

(1990):

$$\overline{r_w} = \frac{r_w}{2\eta\sqrt{a_z}}\sqrt{\left(1+\eta^2/\delta\right)^2 + \left[\left(\sqrt{k_x/k_y}-\sqrt{k_y/k_x}\right)\frac{\cos\theta_w\cos\theta'\sin\theta'}{\delta}\right]^2} \quad \text{(B-19)}$$

With z_o replaced by $\overline{z_o}$ and r_w replaced by $\overline{r_w}$ in Eq. B-18, the resulting transformation for a 3D anisotropic medium is

$$\left|z_o\right| > \frac{25\,r_w}{2\delta\eta\,a_z^{3/2}}\sqrt{\left(1+\eta^2/\delta\right)^2 + \left[\left(\sqrt{k_x/k_y}-\sqrt{k_y/k_x}\right)\frac{\cos\theta_w\cos\theta'\sin\theta'}{\delta}\right]^2} \quad \text{(B-20)}$$

For a 2D anisotropic medium, $k_x=k_y$ and $\eta=1$; thus Eq. B-20 becomes

$$\left|z_o\right| > \frac{25\,r_w}{2\delta\,a_z^{3/2}}\left(1+1/\delta\right). \quad \text{(B-21)}$$

Next we present the radial-flow equations for a 3D anisotropic medium given by Eqs. 1, 2, and 28–30 for three different cases depending on the wellbore inclination: vertical ($\theta_w=0°$), horizontal ($\theta_w=90°$), and inclined ($0°<\theta_w<90°$).

Vertical Well. For $\theta_w=0°$ we obtain $\delta=1$ from Eq. B-14. Thus, Eqs. B-15–B-17 for this case become identical to Eqs. 3–5 in the main text, presented by Prats for the 2D anisotropic case. This result indicates that one can use Prats' equations and the analysis procedure based on a 2D anisotropic case for determining k_h and k_v for the case of 3D anisotropy.

Horizontal Well. For $\theta_w=90°$ we obtain $\delta=\eta\sqrt{k_v/k_h}$ from Eq. B-14. Thus the intercept b given by Eq. B-15 will be a nonlinear function of k_v, k_h, and η for the case of 3D anisotropy. For a 2D anisotropic medium, $\eta=1$; thus $\delta=\sqrt{k_v/k_h}$ and the intercept b given by Eq. B-15 will be a nonlinear function of k_v and k_h.

Inclined Well. For $0°<\theta_w<90°$ the intercept b given by Eq. B-15 will be a nonlinear function of k_v, k_h, θ_w, and η for the case of 3D anisotropy. For a 2D anisotropic medium, $\eta=1$; thus the intercept b given by Eq. B-15 will be a nonlinear function of k_v, k_h, and θ_w.